



Since January 2020 Elsevier has created a COVID-19 resource centre with free information in English and Mandarin on the novel coronavirus COVID-19. The COVID-19 resource centre is hosted on Elsevier Connect, the company's public news and information website.

Elsevier hereby grants permission to make all its COVID-19-related research that is available on the COVID-19 resource centre - including this research content - immediately available in PubMed Central and other publicly funded repositories, such as the WHO COVID database with rights for unrestricted research re-use and analyses in any form or by any means with acknowledgement of the original source. These permissions are granted for free by Elsevier for as long as the COVID-19 resource centre remains active.



Research paper

Identification and characterization of vp7 gene in *Bombyx mori* cytoplasmic polyhedrosis virus



Lei He^{a,1}, Xiaolong Hu^{a,b,1}, Min Zhu^a, Zi Liang^a, Fei Chen^a, Liyuan Zhu^a, Sulan Kuang^a, Guangli Cao^{a,b}, Renyu Xue^{a,b}, Chengliang Gong^{a,b,*}

^a School of Biology & Basic Medical Science, Soochow University, Suzhou 215123, China

^b National Engineering Laboratory for Modern Silk, Soochow University, Suzhou 215123, China

ARTICLE INFO

Keywords:

BmCPV

VP7

Gene expression

ABSTRACT

The genome of *Bombyx mori* cytoplasmic polyhedrosis virus (BmCPV) contains 10 double stranded RNA segments (S1–S10). The segment 7 (S7) encodes 50 kDa protein which is considered as a structural protein. The expression pattern and function of p50 in the virus life cycle are still unclear. In this study, the viral structural protein 7 (VP7) polyclonal antibody was prepared with immunized mouse to explore the presence of small VP7 gene-encoded proteins in *Bombyx mori* cytoplasmic polyhedrosis virus. The expression pattern of vp7 gene was investigated by its overexpression in BmN cells. In addition to VP7, supplementary band was identified with western blotting technique. The virion, BmCPV infected cells and midguts were also examined using western blotting technique. 4, 2 and 5 bands were detected in the corresponding samples, respectively. The replication of BmCPV genome in the cultured cells and midgut of silkworm was decreased by reducing the expression level of vp7 gene using RNA interference. In immunoprecipitation experiments, using a polyclonal antiserum directed against the VP7, one additional shorter band in BmCPV infected midguts was detected, and then the band was analyzed with mass spectrum (MS), the MS results showed that one candidate interacted protein (VP7 voltage-dependent anion-selective channel-like isoform, VDAC) was identified from silkworm. We concluded that the novel viral product was generated with a leaky scanning mechanism and the VDAC may be an interacted protein with VP7.

1. Introduction

The genome of cytoplasmic polyhedrosis viruses (CPVs) normally consist of 10 dsRNA segments (Payne & Mertens, 1983), however, some CPVs have 11–12 dsRNA segments (Zhao, Liang, Hong, & Peng, 2003a; Zhao, Liang, Hong, Xu, & Peng, 2003b). The genome of *Trichoplusiani* cypovirus type 15 (TnCPV-15) and *Antheraea mylitta* cypovirus type 4 (AmCPV-4) is composed of 11 dsRNA segments (Qanungo, Kundu, Mullins, & Ghosh, 2002; Rao, Carner, Scott, Omura, & Hagiwara, 2003). Each dsRNA segment of BmCPV is composed of a single complete open reading frame (ORF). These open reading frames (ORFs) code for the structural as well as non-structural proteins and polyhedrin. Genome analysis of the BmCPV H and I strains revealed that segment S1, S2, S3, S4, S6 and S7 encode viral structural proteins such as VP1, VP2, VP3,

VP4, VP6 and VP7, while segment S5, S8, S9 and S10 encode non-structural proteins p101 (NSP5), p44 (NSP8), NS5 (NSP9) and polyhedrin, respectively (Cao et al., 2012). The eleventh dsRNA segment was found in the *Bombyx mori* cypovirus type 1 (BmCPV-1), which was termed as small polyhedron gene segment (SP) (Arella, Lavallee, Belloncik, & Furuichi, 1988). The twelfth dsRNA segment was also identified in the BmCPV-1 with novel RNA extraction methods (Nagae, Miyake, Kosaki, & Azuma, 2005). The functions of these newly found dsRNA segments are still undefined. A unique characteristic of the dsRNA viruses including BmCPVs, is their ability to accomplish transcription of the dsRNA segments. 5' end of BmCPV genome was processed by adding cap and methylation that form a cap like structure, mGpppAmpGp, protecting mRNAs from degradation by exonuclease enzymes which cuts uncapped mRNA in a 5' to 3' direction (Furuichi,

Abbreviations: BmCPV, *Bombyx mori* cytoplasmic polyhedrosis virus; RNAi, RNA interference; VDAC, Voltage-dependent anion-selective channel-like isoform; CPVs, Cytoplasmic polyhedrosis viruses; TnCPV-15, *Trichoplusiani* cypovirus type 15; ORF, Open reading frame; NSP, Non-structural proteins; NLS, Nuclear localization signal; DAPI, 4', 6-diamidino-2-phenylindole; Co-IP, Co-Immunoprecipitation; SDS-PAGE, Sodium dodecyl sulfate polyacrylamide gel electrophoresis; SD, Standard deviation; BTV, Bluetongue virus; FMDV, Foot-and-mouth disease virus; NTCB, 2-nitro-5-thiocyanobenzoic acid; DLP, Double-layered particle

* Corresponding author at: School of Biology & Basic Medical Science, Soochow University, Suzhou 215123, China.

E-mail address: gongcl@suda.edu.cn (C. Gong).

¹ These authors contributed equally to this work.

<http://dx.doi.org/10.1016/j.gene.2017.06.048>

Received 27 December 2016; Received in revised form 31 May 2017; Accepted 27 June 2017

Available online 28 June 2017

0378-1119/© 2017 Elsevier B.V. All rights reserved.

1978). All of the dsRNA segments in the genome of BmCPV have the similar conservative sequence (GUUAA.....GUUAGCC) in the end (Kuchino, Nishimura, Smith, & Furuichi, 1982), which were predicted as the recognize signal for RNA transcriptase and replicase, or related with both ribosome and mRNA, or assembly with viral structure (LA, 2001). These conservative sequences were also found in the genome of *Dendrolimus punctatus* (Zhao et al., 2003a; Zhao et al., 2003b).

The size of complete segment 7 (S7) in BmCPV is 1501 bp and its ORF is located at 25–1371 bp, which encode 448 amino acid residue. The prokaryotic expression product is 50 kDa (p50). However, anti-p50 can detect one band with 56 kDa from the BmCPV-1 infected BmN4 cells. By using the same antibody, the bands with 34, 36, 38 and 40 kDa from the virion can be detected (Jin, Peng, Wang, Zhang, & Zhang, 2014). M2 gene of Reovirus serotype 1 encoded protein $\mu 1$ could be cleaved into capsid protein $\mu 1C$, which can interact with S4 gene encoded protein $\sigma 3$ to complete the assembly of the virion (Wiener & Joklik, 1988). It is suggested that p50 of BmCPV might play a vital role in the process of assembly of virion.

In the previous study, BmCPV-SZ genome was cloned and found that VP7 enriched alanine and threonine, and a nuclear localization signal (NLS) (Cao et al., 2012). The analysis of the CPV virion with frozen electron microscope and computer three-dimensional reconstruction technology showed that there are two different sizes of protuberance in the outer surface of the capsid. CPV capsid three-dimensional structure analysis showed that there are several protuberances (large protuberance and small protuberance) in the surface of capsid. It was suggested that p50 is processed by posttranslational modification to form the protuberance for the attachment of the virion to the targeted cells (Cheng et al., 2011). Domain analysis of VP7 showed that it may also have role in nucleic acid binding.

This study highlights the potential role of small VP7 gene-encoded proteins in the life cycle of BmCPV. Three siRNAs targeting the *vp7* gene of BmCPV were designed and synthesized to reveal their interference effects on BmCPV replication in infected silkworm larvae and cells. The expression patterns and potential cleavage sites of VP7 were also investigated with the specific antibody, which were produced by the prokaryotic expression system.

2. Materials and methods

2.1. Cell lines and silkworm larvae

BmN cells of domestic silkworm were cultured in TC-100 medium at 27 °C under standard conditions. The silkworms (strain P50) were cultivated on mulberry leaves at 25 ± 1 °C temperature and 70–85% humidity, respectively, with a photoperiod of 12:12 LD.

2.2. siRNA designing

According to the *vp7* gene (accession number: GQ150538) sequence, three siRNA were designed and termed as *vp7*-siRNA1, *vp7*-siRNA2 and *vp7*-siRNA3 (Shanghai Integrated Biotech Solutions Co., Ltd). Control siRNA was designed with *gfp* gene (accession number: NC_011521.1) sequence and named as siRNA-*gfp* (Table 1).

2.3. Silencing of BmCPV *vp7* gene expression in BmN cells and silkworm larvae

1 × 10⁶ BmN cells were transfected with 2 μg siRNA-*gfp* (control) and three BmCPV *vp7* gene specific siRNAs *vp7*-siRNA1, *vp7*-siRNA2 and *vp7*-siRNA3 (test) using 2 μL liposome. After 24 h of transfection, BmCPV virions prepared by our lab (Zhang et al., 2017) were added into the medium containing BmN transfected cells. After 48 h of infection, the infected cells were collected for the RNA extraction from the control group and test group. Two groups (control and test) were made randomly for third instar larva, followed by four replicates for

Table 1
siRNA sequence.

siRNA name	siRNA name	Sequence
vp7-siRNA1	CPV-S7-1 (Sense)	5'-GCGUUAGCUCUACCAAAUATT-3'
	CPV-S7-1 (Anti-sense)	5'-UAUUUGGUGAGUCUAACGCTT-3'
vp7-siRNA2	CPV-S7-2 (Sense)	5'-GCUUCGACUCCUAGAUUATT-3'
	CPV-S7-2 (Anti-sense)	5'-UAUAUCUAGGAGUCGAAGCTT-3'
vp7-siRNA3	CPV-S7-3 (Sense)	5'-GCAGCAUCAGCUAUGAUUATT-3'
	CPV-S7-3 (Anti-sense)	5'-UAAUCAUAGCUGAUGCUGCTT-3'
siRNA- <i>gfp</i>	GFP-274 (Sense)	5'-GGCUACGUCCAGGAGCGCAC-3'
	GFP-274 (Anti-sense)	5'-UGCGCUCUCCGACGUAGCCUU-3'

each group. 1 μg siRNA was injected into haemolymph of each silkworm. Injected silkworms were fed with BmCPV (4.3 × 10⁹ polyhedron/ml). 48 h later, midguts of the infected silkworms were taken for the RNA isolation.

2.4. Extraction of total RNA and cDNA synthesis

Total RNA was extracted from the third instar larvae and BmN cells, infected with BmCPV, according to the standard protocol. The quantity and quality of RNA was determined with both 260/280 absorbance ratio and gel electrophoresis, respectively. RNA was stored at –80 °C for further experiments. 1 μg of total RNA was used as template in the first-strand cDNA synthesis. Real-time quantitative PCR was performed using SYBR Green dye (Bio-Rad, Hong Kong, China) with C1000 Thermal Cycler System (Bio-Rad, Hercules, CA, USA). The primers for the genes expression analysis are listed in Table 2. The 2^{-ΔΔCT} method was used for determination of relative expression level of the detected genes (Livak & Schmittgen, 2001). Experiments were performed in triplicates for each sample.

2.5. VP7 polyclonal antibody preparation

To prepare polyclonal antibody against VP7 proteins of BmCPV, the cDNA with primers listed in Table 1 was amplified with PCR. The amplified PCR products were ligated into the prokaryotic expression vector pET28(a). The recombinant prokaryotic expression vector pET28(a)-*vp7* (Supplementary Fig. 1A) was transformed into *Escherichia coli* strain BL21 cells and induced with 1 mmol/L isopropyl-β-D-thiogalactopyranoside (IPTG). After 4 h of induction, 1.5 ml of the transformed BL21 cells was collected for the recombinant protein detection. The proteins were detected with sodium dodecyl sulfate-polyacrylamide gel electrophoresis (SDS-PAGE) and western blotting (Supplementary Fig. 1B), using a primary antibody of rabbit anti-6 × His (Sigma) and a secondary antibody of horseradish peroxidase (HRP)-conjugated goat anti-rabbit (Sigma). Recombinant protein (VP7) was purified from the 1 L BL21 cells with Ni-NTA (Ni²⁺-nitrilotriacetate) resin (Invitrogen, Carlsbad, CA) using standard procedure. Mouse was immunized with recombinant protein (VP7) for preparing the VP7 polyclonal antibody. Booster injections were administered according to the manufacturer's instructions. The collected serum was stored at –70 °C.

Table 2
Primers for real-time PCR.

Gene name	Primer name	Sequence
vp7	vp7-F	5'-CAGGCAGAACCGCAACTATC-3'
	vp7-R	5'-GGTGATGCTCGTTCGTGGTGT-3'
vp1	vp1-F	5'-GGTCTCGACGTGAATACCGA-3'
	vp1-R	5'-TCGTCTGCTTCACTAGCACG-3'
β-actin	β-actin-F	5'-AACACCCCGTCTGCTCACTG-3'
	β-actin-R	5'-GGCGAGACGTGTGATTTCT-3'

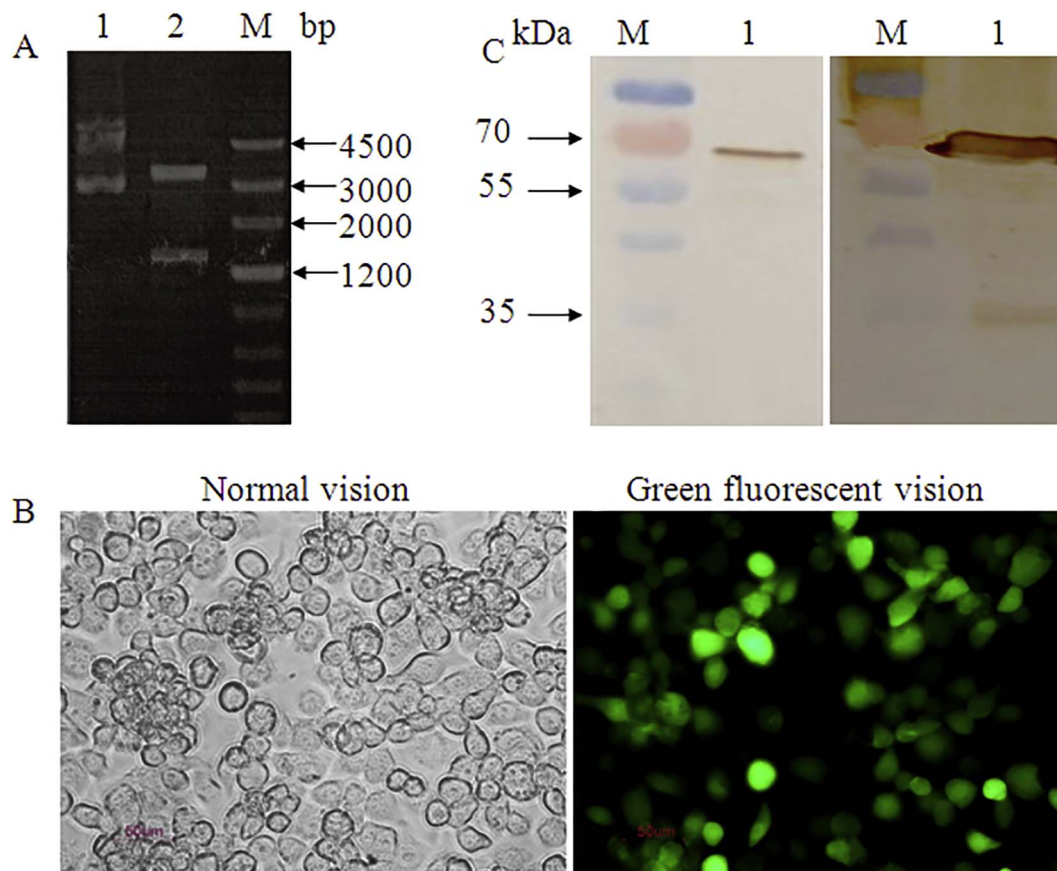


Fig. 1. Overexpression of vp7 gene in BmN cells. (A) Identification of recombinant plasmid pIZT/V5-His-S7 by enzyme digestion. 1, Recombinant plasmid pIZT/V5-His-S7; 2, pIZT/V5-His-S7 by *EcoRI* and *Xba* I. (B) The fluorescent observation of the transgenic cells with transfected with pIZT/V5-His-S7. (C) Identification of recombinant VP7 in transfected BmN cells transfected with pIZT/V5-His-S7. Left, primary antibody was 6*His antibody; Right, primary antibody was VP7 antibody. M. Protein molecular mass marker.

2.6. Overexpression of vp7 gene in BmN cells

pUC-S7 plasmid, preserved in our lab, was used as a template for the amplification of S7 fragment with primers S7-EI/S7-XI. PCR amplicons were digested with digestion enzymes (*EcoRI* and *Xba*) and inserted into the vector pIZT/V5-His to produce a recombinant plasmid pIZT/V5-His-S7. BmN cells were transfected with recombinant plasmid pIZT/V5-His-S7 by adding 2 μ g of recombinant plasmid (pIZT/V5-His-S7) and 5 μ L of liposome into the 25 cm^2 cell culture flask containing BmN cells. After 3 days of transfection, transfected cells were examined with inverted fluorescence microscope for screening transfection in BmN cells. 400 μ g/mL Zeocin antibiotic was added for screening the positive transfected cells. Transfected cells were screened continually for one month using Zeocin antibiotic. 70–80% positive transfected cells were collected for the extraction of total protein.

2.7. Subcellular localization of VP7 in BmCPV infected silkworm larvae midgut

Midguts were derived from BmCPV infected silkworm for the paraffin section. The sections of the midguts were fixed in 4% (v/v) paraformaldehyde at room temperature for 2 h and then rinsed with 0.01 M PBST (10 mM Na_2HPO_4 , 2.7 mM KCl, 140 mM NaCl, 1.8 mM KH_2PO_4 , pH 7.4) containing 0.05% (v/v) Tween-20. The fixed midgut sections were blocked with 3% (w/v) BSA at room temperature for 2 h followed by three washes (5 min each) in PBST, then incubated overnight at 4 $^\circ\text{C}$ with VP7 polyclonal antibody (diluted 1:100 in blocking buffer). After three washes (5 min each) in PBST, cells were incubated with anti-rabbit fluorescein isothiocyanate (FITC)-labeled secondary antibody (HuaAn Biotechnology) at a dilution of 1:200. FITC displays

green fluorescence under blue light. The nuclei were labeled with 4', 6-diamidino-2-phenylindole (DAPI), which exhibits blue fluorescence. Cells were observed under a laser confocal scanning microscope (Nikon, Japan).

2.8. Co-Immunoprecipitation (Co-IP)

Silkworm midgut total proteins were extracted with the RIPA buffer (Sangon, Shanghai). The total proteins were incubated overnight at 4 $^\circ\text{C}$ with the specific murine polyclonal anti-VP7 antibody. The murine un-immune serum was used as the corresponding antibody. Immune complexes were precipitated by adding protein A + G (Sigma), washed three times in the lysis buffer and analyzed by sodium dodecyl sulfate 12% polyacrylamide gel electrophoresis (SDS-PAGE) followed by coomassie brilliant blue staining. Co-IP was replicated three times and all the appeared bands were cut for the mass spectrum. Proteins identification was carried out in Shanghai Applied Protein Technology Co. Ltd.

2.9. Potential cleavage sites prediction

PeptideCutter online software (http://web.expasy.org/peptide_cutter/) was used to predict the potential cleavage sites cleaved by proteases or chemicals in a given protein sequence (Wilkins et al., 1999).

2.10. Statistical analysis

All data are presented as mean \pm standard deviation (SD). Statistical differences were evaluated using Student's *t*-test for unpaired samples. The level of statistical significance was set at * $P < 0.05$, **

$P < 0.01$ and $*** P < 0.001$.

3. Results

3.1. Vp7 gene of BmCPV was overexpressed in the transformed cells

After the successful construction of pIZT/V5-His-S7 expression vector (Fig. 1A), BmN cells were transfected with recombinant vector (pIZT/V5-His-S7) using liposome. 400 $\mu\text{g}/\text{mL}$ Zeocin antibiotic was added for screening the positive transfected cells. After 3 days of transfection, BmN cells were examined with inverted fluorescence microscope. The detection of green fluorescence in transfected cells indicated that expression vector was transferred into the BmN cells. Transfected cells were screened continually for one month using Zeocin antibiotic. The proportion of green fluorescence did not increase after 1 month of zeocin treatment (Fig. 1B). Total protein was extracted from the transfected cells, and VP7 gene expression was confirmed with Western blotting. The results showed that one band with 70 kDa was detected from the transfected cells with 6*His antibody. While, with the VP7 antibody, three bands with about 70, 34 and 35 kDa were detected from the transfected cells (Fig. 1C). VP7 recombinant protein was purified from the transfected cells. The purified product was also confirmed with SDS-PAGE and western blotting. The results showed that only one band with 70 kDa was detected with 6*His antibody, while additional band with 35 kDa was detected by VP7 antibody (Fig. 2A and B).

3.2. Presence of small VP7 gene-encoded proteins in BmCPV infected cultured cells, midgut and BmCPV virion

A novel protein was detected from the overexpression of vp7 gene in the BmCPV infected cultured cells, with VP7 antibody. To identify that whether other proteins could be present in the BmCPV, total proteins were extracted from the BmCPV infected cultured cells (BmN cells), midgut and BmCPV virion. A band with 55 kDa was detected from the BmCPV infected BmN cells using western blotting technique. However, this band is similar with the hypothetical molecular weight of VP7, but smaller than overexpression product in BmN cells. Additional band with 20 kDa was also identified from the BmCPV infected BmN cells (Fig. 3A). Proteins from BmCPV virion were also extracted and detected with VP7 antibody, and four clear bands (55, 38, 25 and 10 kDa) were found in the BmCPV virion (Fig. 3B). Total proteins from the BmCPV infected silkworm midguts (from the first day to the twelfth day) were also extracted, and detected with VP7 antibody. A single positive band was detected from the seventh day of infected silkworm. From the eighth day, three positive bands (55, 25 and 20 kDa) were detected. However, from the ninth to the twelfth day, > 5 bands (55, 28, 25, 20 and 18 kDa) were detected (Fig. 4).

3.3. BmCPV replication can be inhibited by silencing vp7 gene

The expression level of BmCPV vp7 gene after transfection with specific siRNA was evaluated by real-time PCR. Virus replication in transfected cells and silkworm was analyzed. Transfection with siRNA-vp7 reduced the expression level of vp7 gene in infected cells and silkworm compared to the levels of the control (Fig. 5A). The transcript level of vp1 gene was decreased by 15.4 fold. Silencing of the vp7 gene inhibited the multiplication of BmCPV (Fig. 5B). Similar results were obtained from the BmN cells infected with BmCPV. When the expression of vp7 gene was down-regulated in BmN cells, vp1 gene transcript level was decreased by 13 fold (Fig. 5C).

3.4. Short VP7 protein may be translated from alternative in-frame AUG codon in vp7 mRNA

Immunoprecipitation experiments using a polyclonal antiserum directed against the VP7 protein detected the VP7 protein and at least four additional shorter products in infected midguts. These shorter bands were cut for the mass spectrum (Fig. 6), and total 19 proteins were identified. Except VP7, other 18 proteins were encoded by the genome of silkworm. All proteins are listed in the Table 3. Only viral structural protein 7 and voltage-dependent anion-selective channel-like isoform (VDAC) were identified with > 2 unique peptides among all of the identified proteins. These 4 bands with similar molecular weight of the products were identified from the BmCPV virion. It was suggested that these products may be translated from alternative in-frame AUG codon in vp7 mRNA. VDAC was considered a potential interacted protein with the VP7, playing important role in the life cycle of BmCPV.

3.5. VP7 was localized in the cytoplasm of infected midguts

The 3rd instar silkworm larvae were infected with BmCPV. 6 days later, the midguts were extracted to analyze with immunofluorescence technique. The results showed that the viral virion was localized in the cytoplasm of the infected cells (Fig. 7).

4. Discussion

BmCPV genome has ten dsRNA segments (S1–S10), which are encoding structural and non-structural proteins and polyhedrin. Vp7 gene is encoded by the S7 segment, and the function of it is still unclear. In this report, it was demonstrated that 4, 2 and 5 bands of vp7 gene products, recognized by a polyclonal anti-VP7 antibody, are present in BmCPV virion, BmCPV infected cells and BmCPV infected silkworm midguts and 3 bands in transfected cells overexpressed with vp7 gene. These polypeptides appeared may be encoded by a single open reading frame (ORF) produced from the specific AUG codons of vp7 gene. Sequence analysis found that BmCPV vp7 gene contains nearly 17 AUG codons in vp7 ORF. All of these short mRNA encoded > 100 codons, and only 3 short mRNAs were inconsistent with the ORF of vp7 gene.

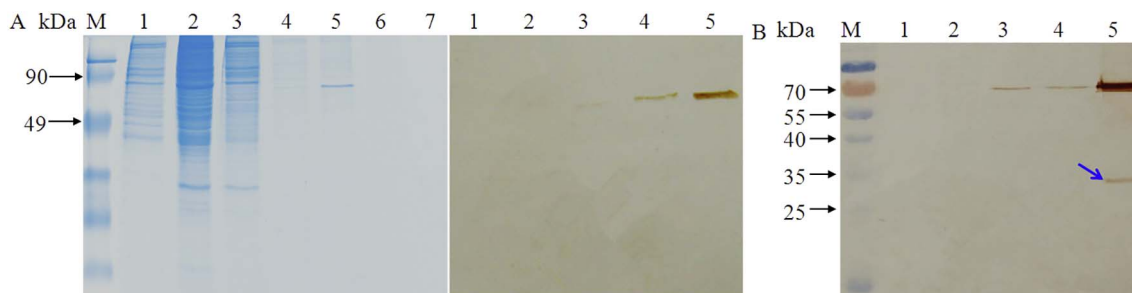


Fig. 2. Various expression patterns of VP7 in transfected cells. (A) Purification of VP7 with Ni^{2+} column chromatography and detection by SDS-PAGE and Western blotting. Primary antibody was 6*His antibody. M. Protein molecular mass marker; 1–7: The purified protein eluted by 10, 20, 50, 100, 200, 300, 400 mmol/L of imidazole solution respectively. (B) Purification of VP7 detected by Western blotting. Primary antibody was VP7 antibody.

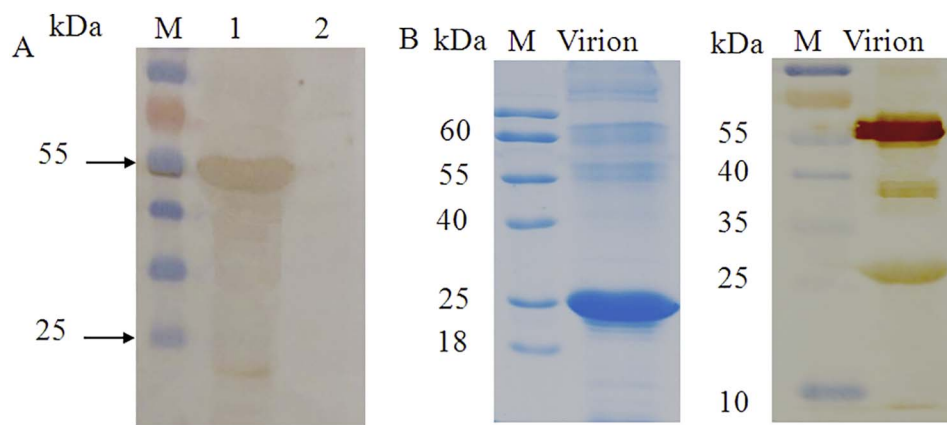


Fig. 3. Identification of VP7 in BmCPV infected cells and BmCPV particle. (A) Identification of VP7 in BmN cells infected with BmCPV. M: Protein molecular mass marker; 1: BmN cells infected with BmCPV particle; 2: BmN cells. (B) Identification of VP7 in BmCPV particle. Primary antibody was VP7 antibody.

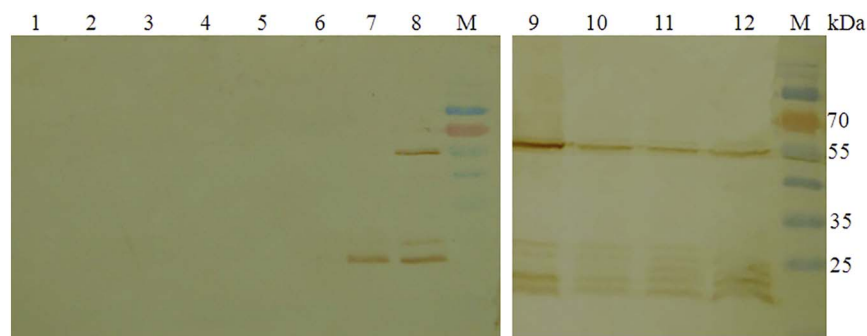


Fig. 4. Detection of VP7 in BmCPV infected silkworm midgut at the different time phase. 1–12. Midguts from 1 d, 2 d, 3 d, 4 d, 5 d, 6 d, 7 d, 8 d, 9 d, 10 d, 11 d and 12 d post infection by BmCPV respectively; M: Protein molecular mass marker.

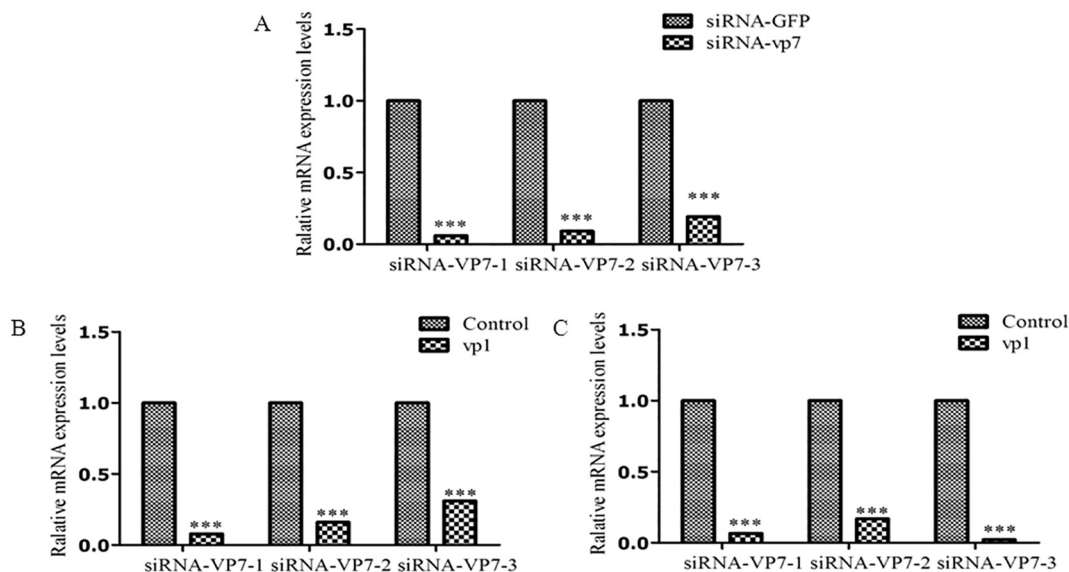


Fig. 5. The relative abundance of *vp7* and *vp1* mRNA in the infected midguts with BmCPV or in BmN cells infected with BmCPV particle. (A) The effect of synthesized siRNAs for the reduction of *vp7* gene. (B) Transfection with siRNA-*vp7* reduced the expression level of *vp7* gene in infected silkworm. (C) Transfection with siRNA-*vp7* reduced the expression level of *vp7* gene in infected cells.

However, we cannot exclude the possibility that these short polypeptides were initiated from non-AUG codons, or truncated VP7 was generated from the cleavage by the proteolytic enzyme. Coding capacity of viruses is enhanced with the evolving overlapping reading frames. Until now, the segmented dsRNA genome of the viruses including Reoviridae, Coronaviruses and Orbivirus families were thought to be monocistronic (i.e. ten genome segments encoding ten proteins), but the identification of novel ORFs, translated in the same reading frame that begin at an alternative downstream AUG, changed this assumption (Gong, Chen, Chen, Kuo, & Shih, 2014). Rice black-streaked dwarf virus genome segments S5, S7 and S9 were bicistronic mRNA, which were involved in

the formation of tubular structures, the formation of viroplasm, virus replication and assembly occurrence. At least 9 novel ORFs were found from the genome of coronaviruses. They were considered as the accessory proteins involved in viral pathogenicity (Shukla & Hilgenfeld, 2015). A small ORF in segment 10, overlapping the NS3 ORF in the +1 position was identified from the genome of bluetongue virus (BTV) (Stewart et al., 2015).

In this study, we concluded that short products of VP7 were appeared in the gels, which might play a significant role in BmCPV life cycle. Further experiments on these short VP7 products will be carried out in our future studies. Voltage-dependent anion channels belongs to

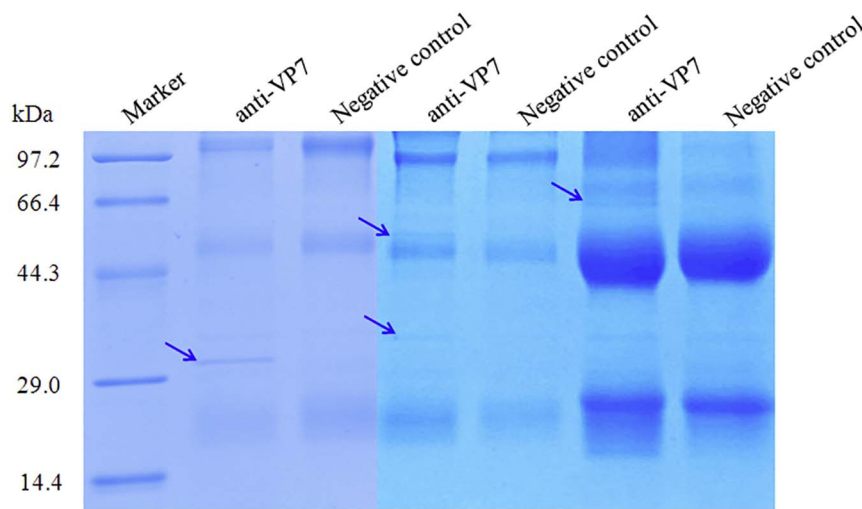


Fig. 6. Identification of the interaction proteins with the BmCPV VP7 with Co-Immunoprecipitation. Co-IP was replicated with three time and all the disparity bands were cut for the mass spectrum.

Table 3
Detection of the proteins in the infected midguts with BmCPV by mass spectrometric analysis.

Protein name	Sequence of detected peptide	UniProtKB no.	MW (Da)	pI	UniquePep count	Cover percent	Structural domains																																							
Voltage-dependent anion-selective channel-like isoform X1/X4/X5	K.ANDVFSK.G	tr H9JHF8	30,076.59	6.96	12	49.29%	–																																							
	K.DFGGSIYQK.V																																													
	K.KANDVFSK.G																																													
	K.NNFALGYQSGDFALHTNVDNGK.D																																													
	K.SESGVEFTSGITSNQESGK.V																																													
	K.SLIGLGYQQK.L																																													
	K.TKSESGVEFTSGITSNQESGK.V																																													
	K.VSDKLDCGVSMK.W																																													
	K.VTLEGTAFAPQTGTK.T																																													
	K.WNTDNTLATDITIQQDK.I																																													
Uncharacterized protein (Myosin-IIIa-like)	K.WTAGSADTLFGVGAK.Y	tr H9J1R7	179,333.79	9.37	1	0.38%	S_TKc MYSc IQ Gp_dh_N																																							
	K.YALDQDASLHAK.I																																													
	K.SKVFLK.Y																																													
	K.AGAEYVVESTGVFTTTDK.A	tr Q1EPM0						35,428.41	7.7	1	5.42%																																			
	K.AM*LKLNPYAAVLKR.K	tr H9IX17										48,779.68	11.58	1	3.23%	–																														
	K.CLELFEELAEDK.E	tr Q9BLC5															82,422.39	4.99	1	1.68%	HATPase_c																									
	K.DLKQLSQKTGLPK.R	tr F2Z897																				44,705.15	8.96	1	3.27%	LIM HOX																				
	K.ILENKNRLLNVK.R	tr B9X256																									71,823.18	8.12	1	1.91%	CAF1 RNA_bind															
	K.KSAISQVASSFSK.D	tr H9JN75																														193,837.45	5.4	1	0.75%	TSP1										
	K.LAVNMVFPFR.L	tr Q8T8B2																																			50,214.47	4.75	1	2.24%	Tubulin Tubulin_C					
K.LDNNGAALVTTLK.G	tr H9J0K5	42,453.67	7.85	1	3.39%	WD40 FYVE																																								
K.LGDDGKKHWHITK.W	tr C4TQH4						26,214.18																																			6.23	1	5.51%	JHBP	
K.PKSAKTIVQQPSVK.A	tr H9JYF7																																													39,396.12
K.PYNTAK.L	tr D7F176							123,398.41	9.72	1	0.57%																																			
K.VTEVLLAAVYK.A	tr Q1HPN7											39,653.3	8.38	1	3.02%	Glycolytic																														
K.YNLNKVM*LYSNK.I	tr H9JNH9																135,134.51	5.48	1	1.01%	LRR_TYPLRRCT LRRNT LRR TIR																									
R.LPDM*SLNFSRITNVR.P	tr H9J1Q6																					123,222.46	6.54	1	1.32%	BRCT																				
R.LTSSLNSIENGK.L	tr H9JY70																										46,203.59	8.64	1	2.91%	ChtBD2															
R.VLVLVVGNTQKK.V	tr H9JD62																															41,605.74	6.86	1	3.13%	GHMP_kinases_N										
K.FDSWEGSLISLSR.D	tr C6K2M8																																				49,853.34	5.52	9	21.43%	PHB HTH					
K.FLQLTFTR.W																																														
K.GLSPIALAQK.K																																														
K.LGNASTPR.Y																																														
R.AKFDSEWEGSLISLSR.D																																														
R.DVVNWK.I																																														
R.LSALALPNTSAR.L																																														
R.NDGTNATPTQFLQLLSYEATENELVK.K																																														
R.VIEYIGVNSM*R.T!																																														
R.VLEYIGVNSM*R.T																																														

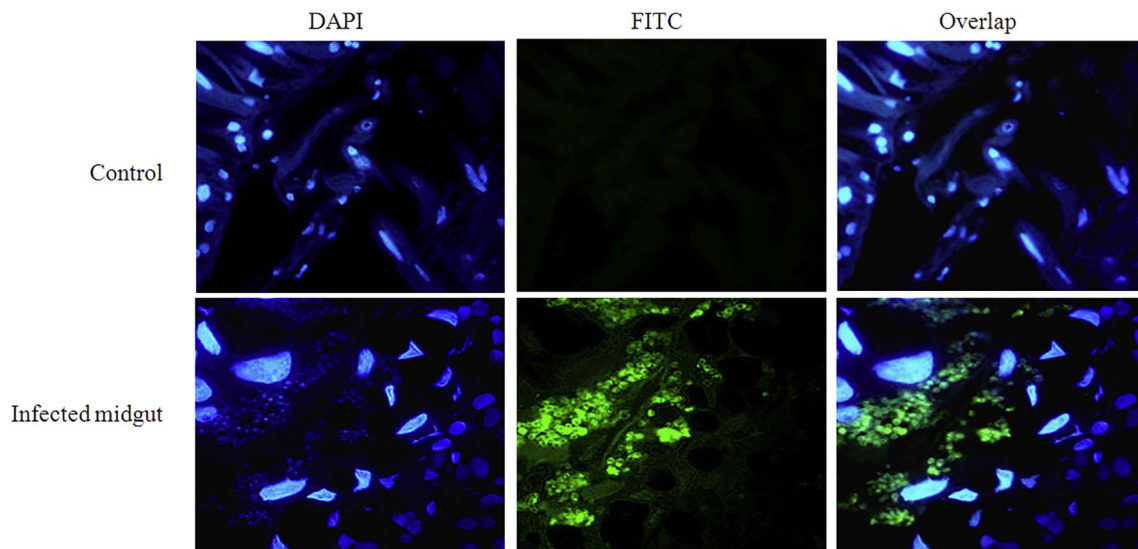


Fig. 7. Immunofluorescence analysis of VP7 in the infected midguts with BmCPV. Control, midguts extracted from normal silkworms. Infected midguts were extracted from the BmCPV infected silkworm.

Table 4
Potential enzymes cleave the sequence predicted with the PeptideCutter online software.

Name of enzyme	No. of cleavages	Positions of cleavage sites
BNPS-Skatole	4	182 196 290 383
Iodosobenzoic acid	4	182 196 290 383
Caspase1	1	148
NTCB (2-nitro-5-thiocyanobenzoic acid)	1	205

a class of porin ion channel and positioned on the outer mitochondrial membrane (Hoogenboom, Suda, Engel, & Fotiadis, 2007). It act as a general diffusion pore for small hydrophilic (water attractant) molecules (Benz, 1994) and helps in the exchanging of ions and molecules between mitochondria and cytosol and is regulated by the interactions with other proteins and small molecules (Hiller, Abramson, Mannella, Wagner, & Zeth, 2010). VDAC has been shown to play a significant role in apoptosis. During apoptosis, increased permeability of VDAC allows for the release of apoptogenic factors (Tsujiimoto & Shimizu, 2002). VDAC-like protein in *Rhipicephalus microplus* may play important role in the infection of *Babesia bigemina* (Rodriguez-Hernandez et al., 2012). Previous studies suggested the apoptosis induction is carried out by the upregulation of VDAC which results in enhanced permeability of outer mitochondrial membrane. The possible reason is thought to be a shift in the VDAC equilibrium to an oligomeric form of the protein which forms large pores and thus allows the release of pro-apoptotic proteins (Ghosh, Pandey, Maitra, Brahmachari, & Pillai, 2007). Furthermore, many viruses encode proteins that act on VDAC to control apoptosis in infected cells (Boya et al., 2003), such as Influenza A and Hepatitis B viruses (Boya et al., 2004). Whether VDAC function is important during *Babesia bigemina* invasion, propagation or replication must be determined in the near future. In the later period of BmCPV infected silkworm larvae, nearly 5 bands were found from the midguts. The alternative hypothesis was that VP7 was produced by the proteolytic enzyme. In our previous study, the analysis of VP5, encoded by the S5 fragment of BmCPV, showed that it has *Foot-and-mouth disease virus* (FMDV) 2A^{pro}-like protease domain which is a short polypeptide of 16 amino acids. The function of this domain is in breaking of the polyprotein of FMDV at the 2A/2B junction co-translationally. This cleavage occurs at its carboxyl terminus at a glycineproline amino acid pair (Ryan, King, & Thomas, 1991; Mattion, Harnish, Crowley, & Reilly, 1996). Whether it might be taking part in the cleavage of the VP7 still

need further investigation. Approximately 5% of gag gene (such as lentiviruses, human immunodeficiency virus, simian immunodeficiency virus) produced other proteins causing by the ribosomal frameshift with independent functions (Rue, Roos, Tarwater, Clements, & Barber, 2005). Two mechanisms for generating more than one protein from a single mRNA have been reported. One possibility is through leaky scanning, such as paramyxoviruses (Kozak, 1989) and Rabies virus. The other possibility is a cap-independent mechanism, such as picornavirus polyprotein and Sendai virus proteins (Pelletier & Sonenberg, 1988; Curran & Kolakofsky, 1989). Why VP7 existed various protein expression patterns among virion, infected cells and larvae? PeptideCutter online software was used to predict the potential cleavage sites cleaved by proteases in VP7. BNPS-Skatole, Iodosobenzoic acid, NTCB (2-nitro-5-thiocyanobenzoic acid) and Caspase1 were predicted to be the potential enzymes (Table 4). In the future, to better understand the potential cleavage mechanisms of VP7, these proteins with small molecular weight will be purified from the BmCPV virion and then will be identified with the mass spectrum analysis.

In this study, we also conducted the experiments for revealing the function of vp7 gene in the viral life cycle. Down-regulated vp7 gene transcript level decreased the transcript level of vp1 gene in BmCPV infected silkworm larvae and BmN cells. It was indicated that vp7 gene was associated with the BmCPV genome replication. The reason for the decline of genome replication due to the reduction in expression level of vp7 gene was that during the cell entry of the progeny virus, the VP7-VP4 outer layer un-coats releasing the intact double-layered particle (DLP) into the cytosol. VP4 mediates cell binding (Fiore, Greenberg, & Mackow, 1991) and membrane disruption (Denisova et al., 1999; Kim, Trask, Babyonyshev, Dormitzer, & Harrison, 2010), but the final steps of DLP delivery require un-coating of VP7 (Cuadras, Arias, & Lopez, 1997; Liprandi et al., 1997). Full un-coating of the outer layer is also required to activate the DLP (Lawton, Estes, & Prasad, 2001), which contains multiple copies of the viral polymerase complex that synthesize and extrude mRNA transcribed from each of the 10 genome segments. The vp7 transcript was reduced because the VP7 layer anchors the VP4 spikes onto the underlying DLP was less, leading to the membrane disruption failure (Chen & Ramig, 1993; Trask & Dormitzer, 2006). The new mRNA transcribed from each segment was decreased, leading to the reduction of the genome replication.

Supplementary data to this article can be found online at <http://dx.doi.org/10.1016/j.gene.2017.06.048>.

Funding

Our work was supported by the National Natural Science Foundation of China (31602007 and 31072085), Natural Science Foundation of Jiangsu Province (BK20140324) and a project funded by the Priority Academic Program of Development of Jiangsu Higher Education Institutions.

Conflict of interest

The authors declare that they have no conflicts of interest.

Ethical approval

This article does not contain any studies with human participants performed by any of the authors.

References

- Arella, M., Lavallee, C., Bellonck, S., Furuichi, Y., 1988. Molecular cloning and characterization of cytoplasmic polyhedrosis virus polyhedrin and a viable deletion mutant gene. *J. Virol.* 62, 211–217.
- Benz, R., 1994. Permeation of hydrophilic solutes through mitochondrial outer membranes: review on mitochondrial porins. *Biochim. Biophys. Acta* 1197, 167–196.
- Boya, P., Roumier, T., Andreau, K., Gonzalez-Polo, R.A., Zamzami, N., Castedo, M., Kroemer, G., 2003. Mitochondrion-targeted apoptosis regulators of viral origin. *Biochem. Biophys. Res. Commun.* 304, 575–581.
- Boya, P., Pauleau, A.L., Poncet, D., Gonzalez-Polo, R.A., Zamzami, N., Kroemer, G., 2004. Viral proteins targeting mitochondria: controlling cell death. *Biochim. Biophys. Acta* 1659, 178–189.
- Cao, G., Meng, X., Xue, R., Zhu, Y., Zhang, X., Pan, Z., Zheng, X., Gong, C., 2012. Characterization of the complete genome segments from BmCPV-SZ, a novel *Bombyx mori* cyovirus 1 isolate. *Can. J. Microbiol.* 58, 872–883.
- Chen, D., Ramig, R.F., 1993. Rescue of infectivity by sequential in vitro transposition of rotavirus core particles with inner capsid and outer capsid proteins. *Virology* 194, 743–751.
- Cheng, L., Sun, J., Zhang, K., Mou, Z., Huang, X., Ji, G., Sun, F., Zhang, J., Zhu, P., 2011. Atomic model of a cyovirus built from cryo-EM structure provides insight into the mechanism of mRNA capping. *Proc. Natl. Acad. Sci. U. S. A.* 108, 1373–1378.
- Cuadras, M.A., Arias, C.F., Lopez, S., 1997. Rotaviruses induce an early membrane permeabilization of MA104 cells and do not require a low intracellular Ca²⁺ concentration to initiate their replication cycle. *J. Virol.* 71, 9065–9074.
- Curran, J., Kolakofsky, D., 1989. Scanning independent ribosomal initiation of the Sendai virus Y proteins in vitro and in vivo. *EMBO J.* 8, 521–526.
- Denisova, E., Dowling, W., LaMonica, R., Shaw, R., Scarlata, S., Ruggeri, F., Mackow, E.R., 1999. Rotavirus capsid protein VP5* permeabilizes membranes. *J. Virol.* 73, 3147–3153.
- Fiore, L., Greenberg, H.B., Mackow, E.R., 1991. The VP8 fragment of VP4 is the rhesus rotavirus hemagglutinin. *Virology* 181, 553–563.
- Furuichi, Y., 1978. “Pretranscriptional capping” in the biosynthesis of cytoplasmic polyhedrosis virus mRNA. *Proc. Natl. Acad. Sci. U. S. A.* 75, 1086–1090.
- Ghosh, T., Pandey, N., Maitra, A., Brahmachari, S.K., Pillai, B., 2007. A role for voltage-dependent anion channel Vdac1 in polyglutamine-mediated neuronal cell death. *PLoS One* 2, e1170.
- Gong, Y.N., Chen, G.W., Chen, C.J., Kuo, R.L., Shih, S.R., 2014. Computational analysis and mapping of novel open reading frames in influenza A viruses. *PLoS One* 9, e115016.
- Hiller, S., Abramson, J., Mannella, C., Wagner, G., Zeth, K., 2010. The 3D structures of VDAC represent a native conformation. *Trends Biochem. Sci.* 35, 514–521.
- Hoogenboom, B.W., Suda, K., Engel, A., Fotiadis, D., 2007. The supramolecular assemblies of voltage-dependent anion channels in the native membrane. *J. Mol. Biol.* 370, 246–255.
- Jin, L., Peng, H., Wang, J.C., Zhang, L.L., Zhang, T., 2014. Advances in the study of infection and transcription mechanism of cytoplasmic polyhedrosis viruses. *Jiangxi Sci.* 32 (4), 509–514.
- Kim, I.S., Trask, S.D., Babyonyshev, M., Dormitzer, P.R., Harrison, S.C., 2010. Effect of mutations in VP5 hydrophobic loops on rotavirus cell entry. *J. Virol.* 84, 6200–6207.
- Kozak, M., 1989. The scanning model for translation: an update. *J. Cell Biol.* 108, 229–241.
- Kuchino, Y., Nishimura, S., Smith, R.E., Furuichi, Y., 1982. Homologous terminal sequences in the double-stranded RNA genome segments of cytoplasmic polyhedrosis virus of the silkworm *Bombyx mori*. *J. Virol.* 44, 538–543.
- LA, N.M.A.S., 2001. Reoviruses and their replication. In: Knipe, D.M., Howley, P.M. (Eds.), *Fields Virology*. Lippincott Williams and Wilkins, Philadelphia, pp. 1679–1728.
- Lawton, J.A., Estes, M.K., Prasad, B.V., 2001. Identification and characterization of a transcription pause site in rotavirus. *J. Virol.* 75, 1632–1642.
- Liprandi, F., Moros, Z., Gerder, M., Ludert, J.E., Pujol, F.H., Ruiz, M.C., Michelangeli, F., Charpilienne, A., Cohen, J., 1997. Productive penetration of rotavirus in cultured cells induces coentry of the translation inhibitor alpha-sarcin. *Virology* 237, 430–438.
- Livak, K.J., Schmittgen, T.D., 2001. Analysis of relative gene expression data using real-time quantitative PCR and the 2^{-ΔΔC_T} method. *Methods* 25, 402–408.
- Mattion, N.M., Harnish, E.C., Crowley, J.C., Reilly, P.A., 1996. Foot-and-mouth disease virus 2A protease mediates cleavage in attenuated Sabin 3 poliovirus vectors engineered for delivery of foreign antigens. *J. Virol.* 70, 8124–8127.
- Nagae, T., Miyake, S., Kosaki, S., Azuma, M., 2005. Identification of novel double-stranded RNA produced in midgut epithelial tissue of the silkworm, *Bombyx mori*, during infection by a cyovirus 1. *J. Insect Biotechnol. Sericol.* 74, 29–34.
- Payne, C.C., Mertens, P.P.C., 1983. Cytoplasmic polyhedrosis viruses. In: Joklik, W.K. (Ed.), *The Reoviridae*. Plenum, New York, N.Y., pp. 425–551.
- Pelletier, J., Sonenberg, N., 1988. Internal initiation of translation of eukaryotic mRNA directed by a sequence derived from poliovirus RNA. *Nature* 334, 320–325.
- Qanungo, K.R., Kundu, S.C., Mullins, J.I., Ghosh, A.K., 2002. Molecular cloning and characterization of *Antheraea mylitta* cytoplasmic polyhedrosis virus genome segment 9. *J. Gen. Virol.* 83, 1483–1491.
- Rao, S., Carner, G.R., Scott, S.W., Omura, T., Hagiwara, K., 2003. Comparison of the amino acid sequences of RNA-dependent RNA polymerases of cyoviruses in the family Reoviridae. *Arch. Virol.* 148, 209–219.
- Rodriguez-Hernandez, E., Mosqueda, J., Alvarez-Sanchez, M.E., Neri, A.F., Mendoza-Hernandez, G., Camacho-Nuez, M., 2012. The identification of a VDAC-like protein involved in the interaction of *Babesia bigemina* sexual stages with *Rhipicephalus microplus* midgut cells. *Vet. Parasitol.* 187, 538–541.
- Rue, S.M., Roos, J.W., Tarwater, P.M., Clements, J.E., Barber, S.A., 2005. Phosphorylation and proteolytic cleavage of gag proteins in budded simian immunodeficiency virus. *J. Virol.* 79, 2484–2492.
- Ryan, M.D., King, A.M., Thomas, G.P., 1991. Cleavage of foot-and-mouth disease virus polyprotein is mediated by residues located within a 19 amino acid sequence. *J. Gen. Virol.* 72 (Pt 11), 2727–2732.
- Shukla, A., Hilgenfeld, R., 2015. Acquisition of new protein domains by coronaviruses: analysis of overlapping genes coding for proteins N and 9b in SARS coronavirus. *Virus Genes* 50, 29–38.
- Stewart, M., Hardy, A., Barry, G., Pinto, R.M., Caporale, M., Melzi, E., Hughes, J., Taggart, A., Janowicz, A., Varela, M., Ratinier, M., Palmarini, M., 2015. Characterization of a second open reading frame in genome segment 10 of bluetongue virus. *J. Gen. Virol.* 96, 3280–3293.
- Trask, S.D., Dormitzer, P.R., 2006. Assembly of highly infectious rotavirus particles re-coated with recombinant outer capsid proteins. *J. Virol.* 80, 11293–11304.
- Tsujimoto, Y., Shimizu, S., 2002. The voltage-dependent anion channel: an essential player in apoptosis. *Biochimie* 84, 187–193.
- Wiener, J.R., Joklik, W.K., 1988. Evolution of reovirus genes: a comparison of serotype 1, 2, and 3 M2 genome segments, which encode the major structural capsid protein mu 1C. *Virology* 163, 603–613.
- Wilkins, M.R., Gasteiger, E., Bairoch, A., Sanchez, J.C., Williams, K.L., Appel, R.D., Hochstrasser, D.F., 1999. Protein identification and analysis tools in the ExPASy server. *Methods Mol. Biol.* 112, 531–552.
- Zhang, Y., Cao, G., Zhu, L., Chen, F., Zar, M.S., Wang, S., Hu, X., Wei, Y., Xue, R., Gong, C., 2017. Integrin beta and receptor for activated protein kinase C are involved in the cell entry of *Bombyx mori* cyovirus. *Appl. Microbiol. Biotechnol.* 101 (9), 3703–3716.
- Zhao, S.L., Liang, C.Y., Hong, J.J., Peng, H.Y., 2003a. Genomic sequence analyses of segments 1 to 6 of *Dendrolimus punctatus* cytoplasmic polyhedrosis virus. *Arch. Virol.* 148, 1357–1368.
- Zhao, S.L., Liang, C.Y., Hong, J.J., Xu, H.G., Peng, H.Y., 2003b. Molecular characterization of segments 7–10 of *Dendrolimus punctatus* cytoplasmic polyhedrosis virus provides the complete genome. *Virus Res.* 94, 17–23.